Geosci. Model Dev. Discuss., doi:10.5194/gmd-2016-89, 2016
Manuscript under review for journal Geosci. Model Dev.
Published: 21 April 2016

Geoscientific Model Development Discussions

Daily black carbon emissions from fires in Northern Eurasia from 2002 to 2013

Wei Min Hao[1*], Alex Petkov[1], Bryce L. Nordgren[1], Robin P. Silverstein[1], Rachel E. Corley[1], Shawn P. Urbanski[1], Nikolaos Evangeliou[2,3], Yves Balkanski[2], and Brad Kinder[4]

[1]Missoula Fire Sciences Laboratory, Rocky Mountain Research Station, United States Forest Service, Missoula, Montana, USA

[2]Laboratoire des Sciences du Climat et de l'Environnement (LSCE), CEA-UVSQ-CNRS UMR 8212, Institut Pierre et Simon Laplace, L'Orme des Merisiers, F-91191 Gif sur Yvette Cedex, France

[3]Norwegian Institute for Air Research (NILU), Department of Atmospheric and Climate Research (ATMOS), Kjeller, Norway

[4]International Program, United States Forest Service, Washington, D.C., USA

[*]Corresponding author: US Forest Service, Rocky Mountain Research Station, Fire Sciences Laboratory, 5775 Highway 10W, Missoula, Montana 59808, USA. T: +1-406-329-4838, F: +1-406-329-4867, whao@fs.fed.us

Abstract

Black carbon (BC) emitted from fires in Northern Eurasia can be transported and deposited on ice and snow in the Arctic and can accelerate its melting during certain times of the year. Thus, we developed a high spatial resolution (500 m × 500 m) dataset to examine daily BC emissions from fires in this region from 2002 to 2013. BC emissions were estimated based on MODIS land cover maps and detected burned areas, the Forest Inventory Survey of the Russian Federation, the IPCC Tier-1 Global Biomass Carbon Map for the year 2000, and biomass specific BC emission factors. Annual BC emissions from Northern Eurasian fires varied greatly, ranging from 0.43 Tg in 2010 to 2.14 Tg in 2013, with an average of 0.82±0.50 Tg from 2002 to 2013. BC emissions from forest fires accounted for about two-thirds of the emissions, followed by grassland fires (15%). Central and Western Asia was the major source region for BC emissions from grassland fires (53%). Russia contributed 83% of the total BC emissions from fires in Northern Eurasia. BC emissions were the highest in the years of 2003, 2008, and 2012. Approximately 57% of the BC emissions from fires occurred in spring (March, April, and May) and 31% in summer. The high emissions in spring also coincide with the most intense period of ice and snow melting in the Arctic.

Geosci. Model Dev. Discuss., doi:10.5194/gmd-2016-89, 2016
Manuscript under review for journal Geosci. Model Dev.
Published: 21 April 2016

Geoscientific Model Development Discussions

1 Introduction

Black carbon (BC), a major component of light absorbing aerosols, is the second most important species for climate forcing after carbon dioxide (Bond et al., 2013). BC absorbs solar radiation, affects radiative forcing, and causes warming of the atmosphere. BC deposited on the Arctic and mountains can accelerate the melting of snow (Flanner et al., 2007). Estimates of BC global sources vary considerably from 2 to 29 Tg yr^{-1} (1 Tg = 10^{12} g) with an average of 7.5 Tg yr^{-1}, according to Bond et al. (2013). Combustion processes in industries and biomass burning are the major sources of BC, with about 64% of the emissions from industries and 36% from biomass burning. BC is an ideal target for mitigation of global warming because of its short atmospheric lifetime of about a week (e.g., Bond et al., 2013).

Deposition of BC on Arctic ice and snow has major effects on global climate. BC deposited on ice and snow absorbs solar radiation that leads to reduced surface albedo, accelerated melting of ice and snow, and increased sea levels (Warren and Wiscombe, 1985; Clarke and Noone, 1985; McConnell et al., 2007). Biomass burning has been identified to be the dominant source of BC in the Arctic during spring (Stohl et al., 2006; Treffeisen et al.,2007; Hegg et al., 2009; Warneke et al., 2009; Hegg et al., 2010; Warneke et al., 2010; Bian et al., 2013), the most prevalent period for snow melting and Arctic Haze events (e.g., Quinn et al., 2007). These fires usually occur in the boreal forests and agricultural lands in Northern Eurasia. BC emitted from boreal forest fires in North America in the summer can also deposit on Arctic snow and reduce surface albedo (Stohl et al., 2006). These findings were based on episodic events observed from airborne campaigns, ground-based monitoring, and dispersion modeling. However, they do not provide the spatial and temporal variability and the amount of BC emitted from various biomass burning sources (e.g., forest, grassland, shrubland, savanna, and cropland). Such information is critical for assessing the impacts of BC on accelerated melting of Arctic ice and snow and on solar radiation in the atmosphere. In addition, BC deposition on the Arctic is further complicated by the dome effects of atmospheric circulation that limits the transport of air mass from lower latitudes into the Arctic (Stohl, 2006). Only certain weather patterns allow the transport of pollutants to the Arctic. It is therefore necessary to develop daily emission sources for the assessment of the transport and deposition of BC on Arctic ice and snow.

In this study, we developed the **F**ire **E**mission **I**nventory –**N**orthern **E**urasia (FEI-NE), a dataset of daily BC emissions from forest, grassland, shrubland, and savanna fires over Northern Eurasia at a 500 m × 500 m resolution from 2002 to 2013. We examined the spatial and temporal variability of BC emissions from fires in different ecosystems in the geopolitical regions of Russia, Eastern Asia, Central and Western Asia, and Europe. The estimates of BC emissions in different regions will assist policy makers in developing effective mitigation policies for reducing BC emissions from fires.

Geosci. Model Dev. Discuss., doi:10.5194/gmd-2016-89, 2016
Manuscript under review for journal Geosci. Model Dev.
Published: 21 April 2016

Geoscientific Model Development Discussions

2 Methods

2.1 Emission calculation

We define Northern Eurasia to encompass Russia, Eastern Asia, Central and Western Asia, and Europe (Fig. 1 inset) covering the region of 35°N–80°N and 10°W–170°W (Fig. 1). Emissions of BC (E) at any spatial and temporal scales are calculated by Eq. (1) (Seiler and Crutzen, 1980; Urbanski et al., 2011):

$$E = A \times FL \times \alpha \times EF \quad (1)$$

where E is the amount of emitted BC, A is the area burned, FL is the fuel loading, α is combustion completeness, and EF is the emission factor for BC. Fuel consumption is calculated as the product of fuel loading and combustion completeness (FL × α). We will discuss the derivation of each parameter in the following sections.

2.2 Burned area

Daily area burned over Northern Eurasia was mapped at a 500 m × 500 m resolution from 2002 to 2013 based on three MODIS (**MOD**erate Resolution **I**maging **S**pectroradiometer) products from NASA Terra and Aqua satellites (Li et al., 2004; Urbanski et al., 2009). The burned area algorithm combines the MODIS thermal anomalies product (MCD14 for Terra and MYD14 for Aqua) at a 1 km resolution four times daily and the MODIS surface reflectance product (MOD02) to map and date burn scars. The burned area mapping method, which was originally developed for the western United States (Urbanski et al., 2011), has two steps. First, a burn scar algorithm is applied to pixels of the surface reflectance product to identify potential burn scars. Then, the potential burn scars are screened for false detections using a contextual filter that eliminates pixels not proximate with recent active fire detections. For mapping burned areas in Northern Eurasia, the burn scar algorithm was unchanged; however, the contextual filter was modified. In this study, potential burn scars not within 5 km and 10 days of active fire detection were classified as false detections and were eliminated. For the western United States the thresholds of the contextual filter were 3 km and 5 days. The algorithms for mapping burned areas in Northern Eurasia have been validated by comparison with Landsat images (Hao et al., 2014). Land cover classification of burned areas was based on the MODIS land cover/land cover change product (MOD12) at a 500 m resolution (Friedl et al., 2010). The date of a burned pixel in FEI-NE was taken as the last date the pixel satisfied the contextual filter.

The burned areas of FEI-NE were compared with the burned areas over Northern Eurasia of Global Fire Emission Dataset (GFED4) and NASA's official burn area product (MCD45) (Fig. 2). Our results agree well with the MCD45 not only in the areas burned but also the interannual variability from 2002 to 2013. However, burned areas of FEI-NE and MCD45 were about 50% higher than the burned areas used in GFED4.

Geosci. Model Dev. Discuss., doi:10.5194/gmd-2016-89, 2016
Manuscript under review for journal Geosci. Model Dev.
Published: 21 April 2016

2.3 Fuel loading

Since limited information was available on the fuel loading for different land cover types over Northern Eurasia, we developed a fuel loading dataset for forested and non-forested areas over Northern Eurasia at a 500 m × 500 m resolution. The data sources were (1) the MODIS land cover map (MOD12, v5), (2) the 2010 land cover map at a 250 m resolution over Russian Federation provided by the Space Research Institute (SRI) of the Russian Academy of Sciences (RAS), (3) the dominant forest species map for 2010 at a 250 m resolution over Russian Federation provided by the SPI, (4) the 2003 Forestry Inventory Survey of Russian Federation, and (5) the IPCC Tier-1 Global Biomass Carbon Map for the year 2000. Fuel loading for forest was categorized into coarse woody debris (CWD), shrub, lower layers, litter, and duff. CWD included fallen logs and branches. Lower layers refer to seedlings, dwarf-shrubs, herbs, mosses and lichen (Alexeyev and Birdsey, 1998). Duff layers were measured up to 20 m deep. For each of the 87 oblasts of the Russian Federation, the loading of each fuel component was estimated based on the 2003 Forestry Inventory Survey of the Russian Federation provided by V. Alexeyev at the RAS Sukachev Institute of Forest in Krasnoyarsk, Russia. In addition, the loading of each fuel component over seven fire prone regions (northern, central and southern Krasnoyarsk, Sakha, Irkutsk, Chita, Amur) were further characterized by different ecozones according to Alexeyev and Birdsey (1998). The fuel loading of forested areas beyond the borders of the Russian Federation was extrapolated from the closest land cover types in the Russian Federation.

The fuel loading of non-forested areas at a 1 km ×1 km resolution was derived from the IPCC Tier-1 Global Biomass Carbon Map for the year 2000 (Ruesch and Gibbs, 2008). The data product was based on biomass carbon stored in aboveground living vegetation created using the International Panel on Climate Change (IPCC) Good Practice Guidance for reporting national greenhouse gas inventories (Penman et al., 2003).

2.4 Combustion completeness

Combustion completeness was estimated using the empirical fire effects model CONSUME (Prichard et al., 2006). The CONSUME natural fuel algorithms include predictive equations for the consumption of multiple fuel components: dead woody debris, shrubs and herbaceous vegetation, litter, and duff/organic soil. In addition to mass loadings for the different fuel components, CONSUME requires moisture content of fine woody debris (diameter < 7.6 cm; FMFWD), coarse woody debris (diameter > 7.6 cm; FMCWD), and duff (FMDUFF) as input. In the FEI-NE simulations, we set the fuel moisture values to levels typical of western United States and Canada wildfire season conditions (FMFWD = 10%, FMCWD = 15%, FMDUFF = 40%). The average combustion completeness predicted for forest fuels using the CONSUME algorithms was 72% for dead woody debris, 90% for herbaceous and shrub fuels, and 58% for combined litter and duff. As a check on the assumed fuel moistures used in our consumption calculations, we used the WFDEI meteorological forcing dataset (Weedon et al., 2014) to estimate FMFWD and FMCWD using the National Fire Danger Rating System basic equations

Geosci. Model Dev. Discuss., doi:10.5194/gmd-2016-89, 2016
Manuscript under review for journal Geosci. Model Dev.
Published: 21 April 2016

(Cohen and Deeming, 1985). We found the areas impacted by fire in Russia had average values of FMFWD = 6% and FMCWD = 12%. To gauge the sensitivity of the fuel consumption estimates to the fuel moisture content we conducted a set of simulations with fuel moisture set at twice our best estimate values. The effect was to reduce combustion completeness to 56% for dead woody debris and 50% for litter and duff. The amount of the fuel burned, or fuel consumption, was estimated as the product of fuel loading and combustion completeness.

2.5 Emission factors

Limited information is available on the emission factors of BC from biomass burning in Northern Eurasia. Therefore, we used emission factors for refractory BC (rBC) from aircraft measurements of emissions from different types of fuels in the United States (May et al., 2014). The rBC was the refractory material in the absorbing aerosol measured by the Single Particle Soot Photometer (SP2). The emission factors for rBC used for estimation of BC emissions were 0.93 g kg^{-1} and 1.36 g kg^{-1} for forest and non-forest fires, respectively.

3 Results

In this section, we present the spatial (500 m, regional, continental) extent and temporal (daily, annual) variability of BC emissions from biomass burning in Northern Eurasia from 2002 to 2013. In addition, the BC emissions from fires over different land cover types and geographic regions are also shown.

3.1 Spatial distribution of BC emissions

The spatial distribution of daily BC emissions from biomass burning over Northern Eurasia at a 500 m × 500 m resolution in 2003 is shown in Fig. 1. The year 2003 had the largest area burned during the period of 2002 – 2013. Fig. 3 shows the maps of daily BC emitted from fires in Northern Eurasia at a 500 m × 500 m resolution from 2002 to 2013. Most of the BC was emitted by forest fires in Russia. BC emissions in Russia were prevalent along the Trans-Siberian Railway (Fig. 1). Human activities in the villages along the railway were probably the major cause of the fires. Much lower emissions were produced from grassland fires in Kazakhstan since fuel loading in non-forested areas is substantially lower than that in forested areas, even though it covers large areas burned. The spatial distribution of BC emissions in the grassland areas of Kazakhstan repeated annually, suggesting the grassland was burned frequently as in the African savannas (Fig. 3).

Table 1 summarizes the BC emissions from fires in different land cover types over different geographic regions from 2002 to 2013. During the 12-year period, a total of 9.9 Tg of BC were emitted. Annual BC emissions from fires varied by a factor of five from 0.43 Tg in 2010 to 2.14 Tg in 2003 with an average of (0.82±0.50) Tg. About two-thirds (68%) of the emissions occurred from fires in forest, followed by grassland (15%), savanna (10%), and shrubland (7%). Geographically, approximately 93% of BC emissions from forest fires took place in Russia. For

Geosci. Model Dev. Discuss., doi:10.5194/gmd-2016-89, 2016
Manuscript under review for journal Geosci. Model Dev.
Published: 21 April 2016

Geoscientific Model Development Discussions

BC emissions from grassland fires, 53% was in Central and Western Asia and 35% in Russia. Russia also dominated the BC emissions from savanna fires (85%) and shrubland fires (89%). Overall, Russia accounted for 83% of the total BC emissions from fires in Northern Eurasia, followed by Central and Western Asia (9%).

3.2 Interannual variability of BC emissions

There was significant interannual variability of BC emissions from fires over different land cover types in Northern Eurasia during the 12-year period of 2002 to 2013 (Table 1 and Fig. 4). Annual BC emissions for the peak three years of 2003, 2008, and 2012 were 2.14, 1.35, and 1.12 Tg, respectively, which were 196%, 64%, and 36% above the 12-year mean BC emissions for the respective years. There is a distinct declining trend of BC emissions for the three peak years during the 12-year period.

The interannual variability of BC emissions for different land cover types followed the same variability as for the total emissions. BC emissions from forest fires accounted for ~ 70% of the total emissions for each of the three peak years. Grassland fires were the second largest source of BC from biomass burning, contributing to ~11% of the total BC emissions for the peak years. There were no apparent trends of BC emissions from fires in different land cover types, except forested areas, in Northern Eurasia during the 12-year period.

3.3 Seasonality

Daily BC emissions in Northern Eurasia for each year of 2002 to 2013 are shown in Fig. 5. The beginning and end of BC emission periods were different for each year. For the 12 years, on average about 57% was emitted in spring (March, April, May), 31% in summer (June, July, August), 11% in fall (September, October, November), and 1% in winter (December, January, February). The major period of emissions from forest fires occurred from late March to late May (Fig. 6a), which coincides with the forest fire season in Russia. This period also corresponds to the latest part of the Arctic Haze phenomena that favors the transport of emissions from lower latitudes to the Arctic region (Quinn et al., 2007). The spring time is also the most effective period for BC emissions to accelerate ice and snow melting in the Arctic (Bond et al., 2013). BC emissions from grassland fires have bimodal distributions from early March to late June and from late August to the end of October (Fig. 6b).

4 Discussion

We present the spatial and temporal distribution of BC emissions from biomass burning over Northern Eurasia at a 500 m × 500 m resolution from 2002 to 2013 in Fig. 3. The results are essential for modeling air quality and ice and snow melting in the Arctic region. The dataset has been utilized for studying the transport and deposition of BC on the Arctic during the 12-year period (Evangeliou et al., 2015).

Geosci. Model Dev. Discuss., doi:10.5194/gmd-2016-89, 2016
Manuscript under review for journal Geosci. Model Dev.
Published: 21 April 2016

Geoscientific Model Development Discussions

4.1 Emission inventory

Biomass burning in Northern Eurasia is a significant source of the global BC emission inventory. The annual mean of BC emissions in this region from 2002 to 2013 was (0.82±0.50) Tg yr^{-1}. The average annual emissions of BC from all the sources globally were estimated to be 7.5 Tg yr^{-1} in the year 2000, in which 4.8 Tg yr^{-1} were from industries and 2.7 Tg yr^{-1} from biomass burning (Bond et al., 2013). Hence, vegetation fires in Northern Eurasia contributed about 11% of the global sources of BC and about 30% of the biomass burning source worldwide.

Approximately 8.2±2.7% of the BC emitted by Northern Eurasian fires was deposited on the Arctic ice, accounting for 45–78% of the BC deposition from all the sources (Evangeliou et al., this issue). However, only about 42% of the BC emitted during the spring and summer was deposited on Arctic ice, which is the most effective period for acceleration of ice and snow melting.

We compared our BC emission estimates from biomass burning sources in Northern Eurasia with GFED3 and GFED4. During the 12-year period, the interannual variability of FEI-NE, GFED3, and GFED4 are quite similar, but the amounts of BC emitted are significantly different (Fig. 7). Total BC emissions, excluding agricultural fires, estimated by GFED4 were 35% higher than GFED3 during the period of 2002–2011. However, during the period of 2002–2013, total annual BC emissions estimated by FEI-NE were several times higher than those of GFED4, ranging from twice in 2002 to 5.1 times in 2003, with an average of 3.5 times.

For forested areas, BC emissions estimated by FEI-NE were 2.1 times higher than GFED4 in 2002 and 8.5 times higher in 2004, with an average of about 4 times during the 12-year period (6.7 Tg for FEI-NE vs. 1.6 Tg for GFED4) (Fig. 8a). The differences can be attributed to both the area burned (Fig. 2) and the amount of available biomass burned. The largest relative difference in BC emissions was in non-forested (grassland, shrubland, and savanna) areas (Fig. 8b). The FEI-NE and GFED4 estimates were 3.19 Tg and 0.20 Tg, respectively, for the 12-year period.

4.2 Seasonality

Emissions of BC in the spring time should have the greatest impacts on the melting of ice in the Arctic (Flanner et al., 2007; Flanner et al., 2009; Hegg et al., 2010; Bond et al., 2013), which usually occurred in late March. High BC concentrations in spring have been observed in smoke plumes from aircraft measurements (Warneke et al., 2009, Warneke et al., 2010) and at the ground monitoring station Zellepin in Norway (Stohl et al., 2007). Our estimates of BC emissions were consistent with the observations, being the highest in spring every year from 2002 to 2013, even though the start and end dates of BC emissions from biomass burning varied (Fig. 5). Forest fires dominated the emissions (Fig. 6a). The timing and the magnitude of BC emissions depend on the burned area and fuel conditions that are ultimately determined by weather and human activities.

Geosci. Model Dev. Discuss., doi:10.5194/gmd-2016-89, 2016
Manuscript under review for journal Geosci. Model Dev.
Published: 21 April 2016

Geoscientific Model Development Discussions

4.3 Agricultural vs. non-agricultural fires

One of the key aspects for developing mitigation policies of BC impacts on accelerated ice and snow melting in the Arctic is to understand the contribution of different biomass burning sources for BC, especially the non-agricultural versus agricultural fires. It is much more feasible to control agricultural fires than wildfires. Several episodic events indicated that BC emitted from agricultural fires may be transported to the Arctic. The exceedingly high levels of equivalent BC observed at the Zellepin monitoring station in Norway in early May 2006 have been attributed to the transport of smoke plumes of agricultural fires in Eastern Europe to the European Arctic (Stohl et al., 2007). Smoke plumes from agricultural burning in Kazakhstan and southern Russia in April 2008 have been observed to reach to the western Arctic (Warneke et al., 2009, Warneke et al., 2010; Bian et al., 2013).

The most comprehensive study of BC emissions from agricultural burning in Russia was during the period of 2003 –2009 by McCarty et al. (2012). The annual emissions ranged from 0.002 to 0.022 Tg with an average of 0.009 Tg, in which about 34% was burned in spring. The results are consistent with the unpublished results of Hall, Loboda and Hao for average annual BC emissions of cropland fires in Russia (0.011± 0.003 Tg yr^{-1}) during the period of 2003–2012. Therefore, total annual BC emissions from agricultural fires account for only 1.5% of total BC emissions from fires in Russia, which is an insignificant BC source.

4.4 Russia

One of the objectives of this study was to identify the geographic regions of BC emissions over Northern Eurasia to support the development of mitigation policies. Russia was the dominant region for BC emissions from biomass burning during the 12-year period, accounting for 83% of the total emissions from fires in Northern Eurasia (Table 1). In Russia, 75.6% of the BC emissions occurred in forest, 10.4% in savannas, 7.7% in shrubland, and 6.3% in grassland.

Spring is the most critical season for accelerated melting of ice and snow in the Arctic. Spring fires accounted for an average of 53.0±15.2% of the annual BC emissions in Russia during the 12-year period, followed by 12.7±9.2% from fires in the summer.

5 Conclusions

We have estimated daily BC emissions from forest, grassland, shrubland, and savanna fires in different geographic regions over Northern Eurasia at a 500 m ×500 m resolution from 2002 to 2013. The results are essential for modeling the impact of BC on accelerated ice melting in the Arctic and for modeling air quality at high latitudes. During the 12-year period, BC emissions from biomass burning in Northern Eurasia accounted for about 11% of the global BC sources or 30% of the biomass burning source worldwide. Forest fires dominated BC emissions (68%) followed by grassland fires (15%). Russia was the dominant country contributing about 83% of total BC emissions from biomass burning in Northern Eurasia. Approximately 57% of the BC

Geosci. Model Dev. Discuss., doi:10.5194/gmd-2016-89, 2016
Manuscript under review for journal Geosci. Model Dev.
Published: 21 April 2016

emissions occurred in spring time, when the greatest impact occurred on ice and snow melting in the Arctic. Our estimates of BC emissions from biomass burning were about 3.5 times higher than the GFED4 estimates. Additional atmospheric measurements of BC in regions where fires contribute the most BC emissions coupled with the modeling of atmospheric transport and deposition should help in determining which of these estimates best represent BC emissions.

Acknowledgements

We thank Vlady Alexeyev at the Sukachev Institut of Forest and Sergey Bartalev at the Space Research Institute of the Russian Academy of Sciences to provide the essential datasets for mapping the fuel loading. This project was supported by the US Department of State, US Forest Service Research and Development, and NASA Terrestrial Ecology Program.

6 References

Alexeyev, V. A., Birdsey, R. A. [Editors]: Carbon storage in forests and peatlands of Russia. Gen. Tech. Rep. NE-244. Radnor, PA: U.S. Department of Agriculture, Forest Service, Northeastern Research Station. 137 p., 1998.

Bian, H., Colarco, P. R., Chin, M., Chen, G., Rodriguez, J. M., Liang, Q., Blake, D., Chu, D. A., da Silva, A., Darmenov, A. S., Diskin, G., Fuelberg, H. E., Huey, G., Kondo, Y., Nielsen, J. E., Pan, X., and Wisthaler, A.: Source attributions of pollution to the Western Arctic during the NASA ARCTAS field campaign, Atmos. Chem. Phys., 13, 4707-4721, doi:10.5194/acp-13-4070-2013, 2013.

Bond, T. C., Doherty, S. J., Fahey, D. W., Forster, P. M., Berntsen, T., DeAngelo, B. J., Flanner, M. G., Ghan, S., Kärcher, B., Koch, D., Kinne, S., Kondo, Y., Quinn, P. K., Sarofim, M. C., Schultz, M. G., Schulz, M., Venkataraman, C., Zhang, H., Zhang, S., Bellouin, N., Guttikunda, S. K., Hopke, P. K., Jacobson, M. Z., Kaiser, J. W., Klimont, Z., Lohmann, U., Schwarz, J. P., Shindell, D., Storelvmo, T., Warren, S. G., and Zender C. S.: Bounding the role of black carbon in the climate system: A scientific assessment, J. Geophys. Res. Atmos., 118, 5380–5552, doi:10.1002/jgrd.50171, 2013.

Clarke, A. D. and Noone, K. J.: Soot in the Arctic snowpack: A cause for perturbations in radiative transfer, Atmos. Environ., 19, 2045-2053, 1985.

Geosci. Model Dev. Discuss., doi:10.5194/gmd-2016-89, 2016
Manuscript under review for journal Geosci. Model Dev.
Published: 21 April 2016

Cohen, J. D. and Deeming, J. E.: The National Fire Danger Rating System: basic equations, Gen. tech. Rep. PSW-82, Pacific Southwest Forest and Range Experiment Station, Forest Service, U.S. Department of Agriculture, Berkeley, CA, 16 pp., available at: http://www.treesearch.fs.fed.us/pubs/27298, 1985.

Evangeliou, N., Balkanski, Y., Hao, W. M., Petkov, A., Silverstein, R. P., Corley, R., Nordgren, B. L., Urbanski, S. P., Eckhardt, S., Stohl, A., Tunved, P., Crepinsek, S., Jefferson, A., Sharma, S., Nøjgaard, J. K., and Skov, H.: Wildfires in Northern Eurasia affect the budget of black carbon in the Arctic. A 12-year retrospective synopsis (2002-2013), Atmos. Chem. Phys. Discuss., doi:10.5194/acp-2015-994, in review, 2016.

Flanner, M. G., Zender, C. S., Randerson, J. T., and Rasch, P. J.: Present-day climate forcing and response from black carbon in snow, J. Geophys. Res., 112, D11202, doi:10.1029/2006JD008003, 2007.

Flanner, M. G., Zender C. S., Hess, P. G., Mahowald, N. M., Painter, T. H., Ramanathan, V., and Rasch, P. J.: Springtime warming and reduced snow cover from carbonaceous particles, Atmos. Chem. Phys., 9(7), 2481–2497, 2009.

Friedl, M. A., Sulla-Menashe, D., Tan, B., Schneider, A., Ramankutty, N., Sibley, A., and Huang, X.: MODIS Collection 5 global land cover: algorithm refinements and characterization of new datasets, Remote Sens. Environ. 114, 168-182, doi:10.1016/j.rse.2009.08.016, 2010.

Hao, W. M., Nordgren, B., Petkov, A., Corley, R. E., Urbanski, S. P.; Comparison of MODIS-derived burned area algorithm with Landsat images in eastern Siberia, Russia, 2012 International Emission Inventory Conference: Emission Inventories – Meeting the Challenges Posed by Emerging Global, National, Regional and Local Air Quality Issues, Tampa, FL, 13–16 August, 2012.

Hegg, D. A., Warren, S. G., Grenfell, T. C., Doherty, S. J., Larson, T. V., Clarke, A. D.: Source attribution of black carbon in Arctic snow, Environ. Sci. Technol., 43, 4016-4021, 2009.

Geosci. Model Dev. Discuss., doi:10.5194/gmd-2016-89, 2016
Manuscript under review for journal Geosci. Model Dev.
Published: 21 April 2016

Hegg, D. A., Warren, S. G. Grengell, T.C. Doherty, S. J., and Clarke, A. D.: Source of light-absorbing aerosol in Arctic snow and their seasonal variation, Atmos. Chem. Phys., 10-10923-10928, doi:10.5194/acp-10-10923-2010, 2010.

Li, R.-R., Kaufman, Y. J., Hao, W. M., Salmon, J. M., and Gao, B.-C.: A technique for detecting burn scars using MODIS data, IEEE Trans. Geosci. Remote Sens., 42, 1300-1308, 2004.

May, A. A., McMeeking, G. R., Lee, T., Taylor, J. W., Craven, J. S., Burling, I., Sullivan, A. P., Akagi, S., Collett Jr., J. L., Flynn, M., Coe, H., Urbanski, S. P., Seinfeld, J. H., Yokelson, R. J., and Kreidenweis, S. M.: Aerosol emissions from prescribed fires in the United States: a synthesis of laboratory and aircraft measurements, J. Geophys. Res. Atmos.,119, doi:10.1002/2014JD021848, 2014.

McCarty, J. L., Ellicott, E. A., Romanenkov, V., Rukhovitch, D., and Koroleva, P.: Multi-year black carbon emissions from cropland burning in the Russian Federation, Atmos. Environ., 63, 223-238, 2012.

McConnell, J. R., Edwards, R., Kok, G. L., Flanner, M. G., Zender, C. S., Saltzman, E. S., Banta, J. R., Pasteris, D. R., Carter, M. M., and Kahl, J. D.: 20th-century industrial black carbon emissions altered Arctic climate forcing, Science, 317-1381-1384, 2007.

Penman, J., Gytarsky, M., Hiraishi, T., Krug, T., Kruger, D., Pipatti, R., Buendia, L., Miwa, K., Ngara, T., Tanabe, K., Wagner, F.: Good practice guidance for land use, land-use change and forestry. IPCC National Greenhouse Gas Inventories Programme and Institute for Global Environmental Strategies, Kanagawa, Japan. Available at: http://www.ipcc-nggip.iges.or.jp/public/gpglulucf/gpglulucf_contents, 2003.

Prichard, S. J., Ottmar, R. D., and Anderson, G. K.: Consume 3.0 user's guide, Pacific Northwest Research Station, Corvallis, Oregon, 234 pp., available at: http://www.firelab.org/science-applications/fire-fuel/111-fofem, 2006.

Quinn, P. K., Shaw, G., Andrews, E., Dutton, E. G., Ruoho-Airola, T., and Gong, S. L.: Arctic haze: current trends and knowledge gaps, Tellus B, 59, 99-114, doi: 10:.1111/j.1600-0889.2006.00238.x, 2007.

Ruesch, A., and Gibbs, H. K.: New IPCC Tier-1 Global Biomass Carbon Map for the Year 2000. Available online from the Carbon Dioxide Information Analysis Center [http://cdiac.ornl.gov], Oak Ridge National Laboratory, Oak Ridge, Tennessee, 2008.

Seiler, W. and Crutzen, P. J.: Estimates of gross and net fluxes of carbon between the biosphere and the atmosphere from biomass burning, Climatic Change, 2, 207-247, 1980.

Stohl, A., Andrews, E., Burkhart, J. F., Forster, C., Herber, A., Hoch, S. W., Kowal., D., Lunder, C., Mefford, T., Ogren, J. A., Sharma, S., Spichtinger, N., Stebel, K., Stone, R., Ström, J., Tørseth, K., Wehrli, C., and Yttri, K. E.: Pan-Arctic enhancements of light absorbing aerosol concentrations due to North American boreal forest fires during summer 2004, J. Geophys. Res., 111, D22214, doi:10.1029/2006JD007216, 2006.

Stohl, A., Characteristics of atmospheric transport into the Arctic troposphere, J. Geophys. Res. 111, D11306, doi:10.1029/2005JD006888, 2006.

Stohl, A., Berg, T., Burkhart, J. F., Fjæraa, A. M., Forster, C., Herber, A., Hov, Ø., Lunder, C., McMillan, W. W., Oltmans, S., Shiobara, M., Simpson, D., Solberg, S., Stebel, K., Ström, J., Tørseth, K., Treffeisen, R., Virkkunen, K., and Yttri, K. E.: Arctic smoke – record high air pollution levels in the European Arctic due to agricultural fires in Eastern Europe in spring 2006, Atmos. Chem. Phys., 7, 511-534, doi:10.5194/acp-7-511-2007, 2007.

Treffeisen, R., Tunved, P., Ström, J., Herber, A., Bareiss, J., Helbig, A., Stone, R. S., Hoyningen-Huene, W., Krejci, R., Stohl, A., and Neuber, R.: Arctic smoke – aerosol characteristics during a record smoke event in the European Arctic and its radiative impact, Atmos. Chem. Phys., 7, 3035-3053, 2007.

Urbanski, S. P., Salmon, J. M., Nordgren, B. L., and Hao, W. M.: A MODIS direct broadcast algorithm for mapping wildfire burned area in the western United States, Remote Sens. Environ., 113, 2511–2526, 2009.

Urbanski, S. P., Hao, W. M., and Nordgren, B.: The wildlandfire emission inventory: western United States emission estimates and an evaluation of uncertainty, Atmos. Chem. Phys. 11, 12973-13000, doi:10.5194/acp-11-12973-2011, 2011.

Geosci. Model Dev. Discuss., doi:10.5194/gmd-2016-89, 2016
Manuscript under review for journal Geosci. Model Dev.
Published: 21 April 2016

Warneke, C., Bahreini, R., Brioude, J., Brock, C. A., de Gouw, J. A., Fahey, D. W., Froyd, K. D., Holloway, J. S., Middlebrook, A., Miller, L., Montzka, S., Murphy, D. M., Peischl, J., Ryerson, T. B., Schwarz, J. P., Spackman, J. R., and Veres, P.: Biomass burning in Siberia and Kazakhstan as an important source for haze over the Alaskan Arctic in April 2008, Geophys. Res. Lett., 36, L02813, doi:10.1029/2008GL036194, 2009.

Warneke, C., Froyd, K. D., Brioude, J., Bahreini, R., Brock, C. A., Cozic, J., de Gouw, J. A., Fahey, D. W., Ferrare, R., Holloway, J. S., Middlebrook, A. M., Miller, L., Montzka, S., Schwarz, J. P., Sodemann, H., Spackman, J. R., and Stohl, A.: An important contribution to springtime Arctic aerosol from biomass burning in Russia, Geophys. Res. Lett., 37, L01801, doi:10.1029/2009GL04816, 2010.

Warren, S. G. and Wiscombe, W. J.: Dirty snow after nuclear war, Nature, 313, 467-470, 1985.

Weedon, G. P., Balsamo, G., Bellouin, N., Gomes, S., Best, M. J., and Viterbo, P.: The WFDEI meteorological forcing data set: WATCH Forcing Data methodology applied to ERA-Interim reanalysis data, Water Resour. Res., 50, 7505–7514, doi:10.1002/2014WR015638, 2014.

Geosci. Model Dev. Discuss., doi:10.5194/gmd-2016-89, 2016
Manuscript under review for journal Geosci. Model Dev.
Published: 21 April 2016

Geoscientific Model Development Discussions

Table Captions

Table 1. Annual BC emissions in different land cover types over different geographic regions in Northern Eurasia from 2002-2013.

Figure Captions

Figure 1. Spatial distribution of BC emissions in Northern Eurasia at a 500 m × 500 m resolution in 2003. The black line illustrates the Trans-Siberian Railway. The insert is the geographic regions of Russia, East Asia, Central and Western Asia, and Europe.

Figure 2. Comparisons of annual burned areas in forests and non-forests over Northern Eurasia mapped by FEI-NE, GFED4 and MCD45.

Figure 3. Daily BC emissions in Northern Eurasia at a 500 m × 500 m resolution from 2002-2013.

Figure 4. Interannual variability of BC emissions for different land cover types in Northern Eurasia from 2002-2013

Figure 5. Daily BC emissions in Northern Eurasia from 2002-2013.

Figure 6. Daily BC emissions in different land cover types in Northern Eurasia from 2002-2013. Note the differences in the Y-axis scales of BC emissions from fires in different land cover types.

Figure 7. Comparisons of annual BC emissions from biomass burning in Northern Eurasia from 2002-2013 estimated by FEI-NE, GFED4, and GFED3.

Figure 8. Comparisons of annual BC emissions from (a) forest and (b) non-forest fires for FEI-NE, GFED4, and GFED3 from 2002-2013.

Geosci. Model Dev. Discuss., doi:10.5194/gmd-2016-89, 2016
Manuscript under review for journal Geosci. Model Dev.
Published: 21 April 2016

Geoscientific Model Development Discussions

Table 1. Annual BC emissions in different land cover types over different geographic regions in Northern Eurasia from 2002-2013.

Region	2002	2003	2004	2005	2006	2007	2008	2009	2010	2011	2012	2013	Total
							Black Carbon Emissions (Gg yr^{-1})						
							Forest						
							(Evergreen Needleleaf, Evergreen Broadleaf, Deciduous Needleleaf, Deciduous Broadleaf, Mixed)						
Russia	412.3	1419.4	277.1	213.0	550.4	274.1	942.1	378.1	222.5	511.8	743.8	281.4	6226.0
East Asia	10.1	67.1	72.7	26.4	22.6	25.5	34.7	57.5	9.4	31.1	25.2	8.7	390.8
Central & Western Asia	0.5	1.4	1.0	0.9	1.3	1.7	2.2	1.6	2.8	0.6	1.5	1.0	16.5
Europe	5.4	13.5	4.8	3.7	5.7	9.5	5.2	4.7	2.1	6.9	12.6	2.8	77.0
Subtotal	428.2	1501.4	355.6	243.9	580.1	310.8	984.3	441.9	236.8	550.4	783.0	293.9	6710.4
							Grassland						
Russia	27.3	112.1	20.5	32.9	56.3	48.1	70.1	37.8	22.1	35.1	40.3	15.4	517.8
East Asia	14.3	20.8	13.6	9.9	12.7	16.5	11.8	12.2	5.8	14.2	23.0	15.9	170.6
Central & Western Asia	62.0	111.8	95.4	59.7	100.8	55.9	78.8	46.8	74.4	22.3	49.9	13.8	771.5
Europe	0.1	0.8	0.1	0.2	0.3	1.2	0.3	0.3	0.1	0.6	0.7	0.2	5.0
Subtotal	103.7	245.4	129.6	102.8	170.1	121.6	161.0	97.1	102.4	72.1	113.9	45.3	1465.0
							Shrubland (Closed Shrubland and Open Shrubland)						
Russia	37.6	191.7	13.3	41.6	25.2	19.1	43.4	41.2	48.9	32.9	73.6	69.6	638.1
East Asia	2.2	2.0	1.0	2.1	4.8	5.3	4.3	6.0	2.0	2.4	10.7	2.1	44.8
Central & Western Asia	0.9	3.7	4.0	1.5	2.0	2.4	1.3	1.2	3.1	0.8	1.3	1.0	23.1
Europe	0.3	1.0	0.4	0.4	0.7	2.8	1.7	0.6	0.3	0.8	1.2	0.4	10.8
Subtotal	41.0	198.4	18.7	45.6	32.7	29.6	50.7	49.0	54.3	36.9	86.8	73.1	716.8
							Savanna (Woody Savanna and Savanna)						
Russia	24.6	177.8	17.6	46.6	62.3	60.3	139.9	41.9	27.0	58.0	120.9	80.4	857.3
East Asia	2.4	7.8	5.5	5.2	11.0	7.4	10.8	9.5	2.9	5.8	8.1	3.6	80.0
Central & Western Asia	0.9	2.7	1.8	2.2	3.6	3.5	3.4	4.8	2.1	1.0	3.1	2.3	31.3
Europe	1.1	3.3	1.3	1.2	1.9	7.5	2.3	3.0	0.9	3.3	6.2	2.4	34.3
Subtotal	29.0	191.6	26.1	55.2	78.8	78.7	156.4	59.1	32.9	68.0	138.3	88.7	1002.9
Total	601.8	2136.9	530.1	447.5	861.6	540.7	1352.4	647.2	426.4	727.5	1122.1	501.0	9895.1

Geosci. Model Dev. Discuss., doi:10.5194/gmd-2016-89, 2016
Manuscript under review for journal Geosci. Model Dev.
Published: 21 April 2016

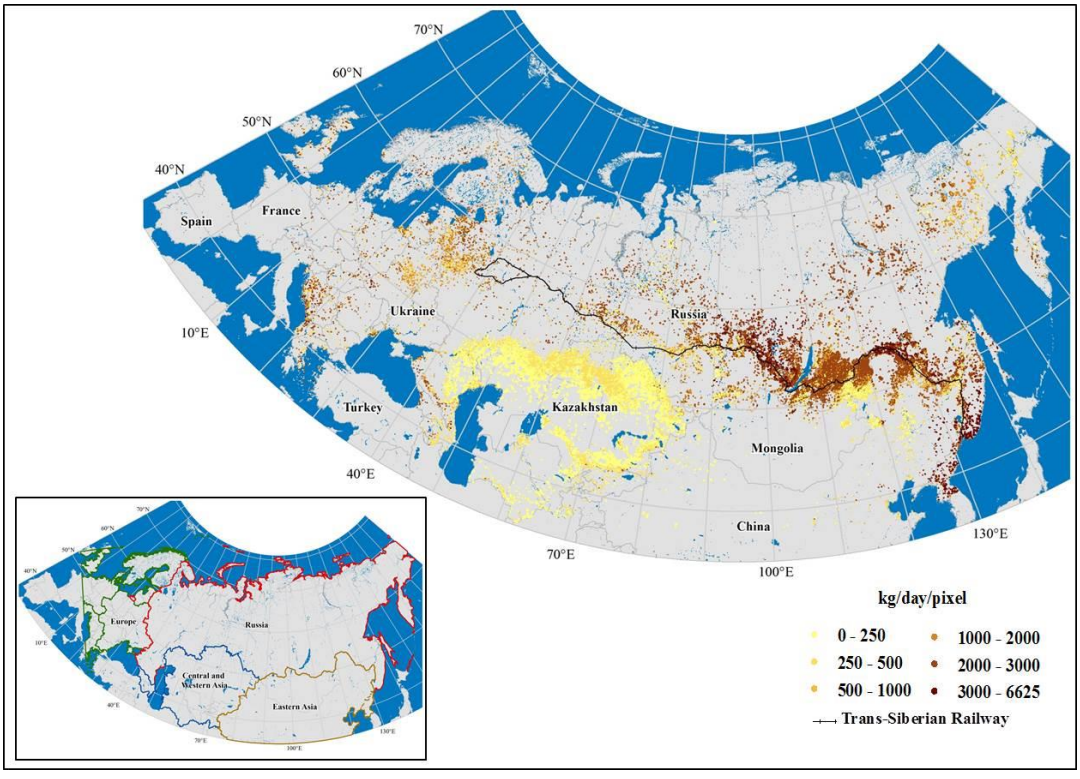

Figure 1. Spatial distribution of BC emissions in Northern Eurasia at a 500 m × 500 m resolution in 2003. The black line illustrates the Trans-Siberian Railway. The inset is the geographic regions of Russia, East Asia, Central and Western Asia, and Europe.

Geosci. Model Dev. Discuss., doi:10.5194/gmd-2016-89, 2016
Manuscript under review for journal Geosci. Model Dev.
Published: 21 April 2016

Geoscientific Model Development Discussions
Open Access
EGU

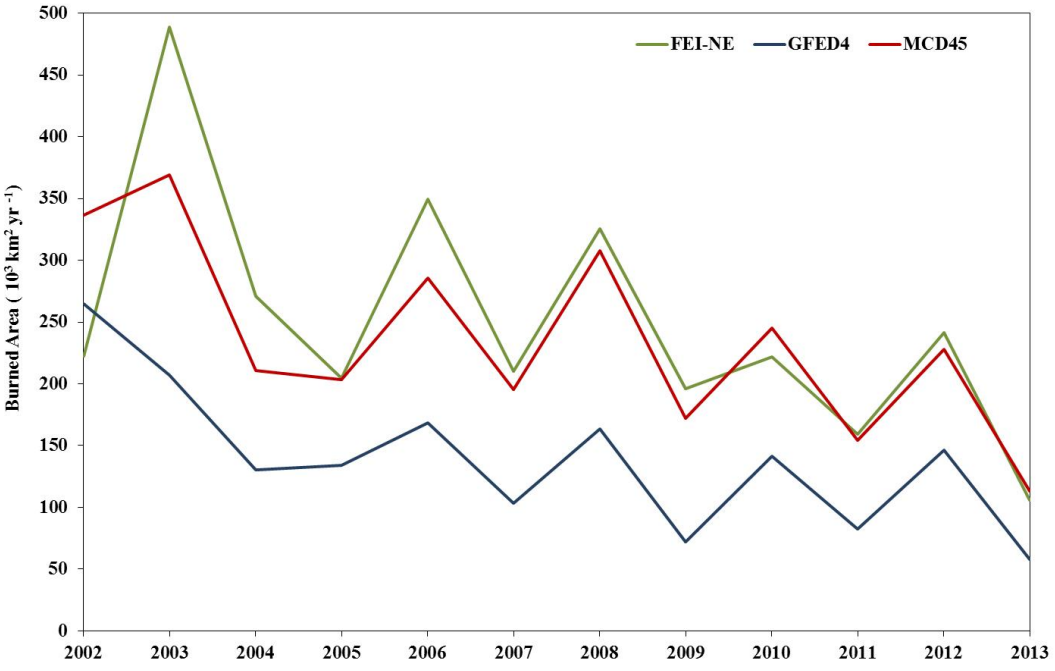

Figure 2. Comparisons of burned areas in forests and non-forests over Northern Eurasia mapped by FEI-NE, GFED4, and MCD45.

Geosci. Model Dev. Discuss., doi:10.5194/gmd-2016-89, 2016
Manuscript under review for journal Geosci. Model Dev.
Published: 21 April 2016

Geoscientific Model Development Discussions
Open Access
EGU

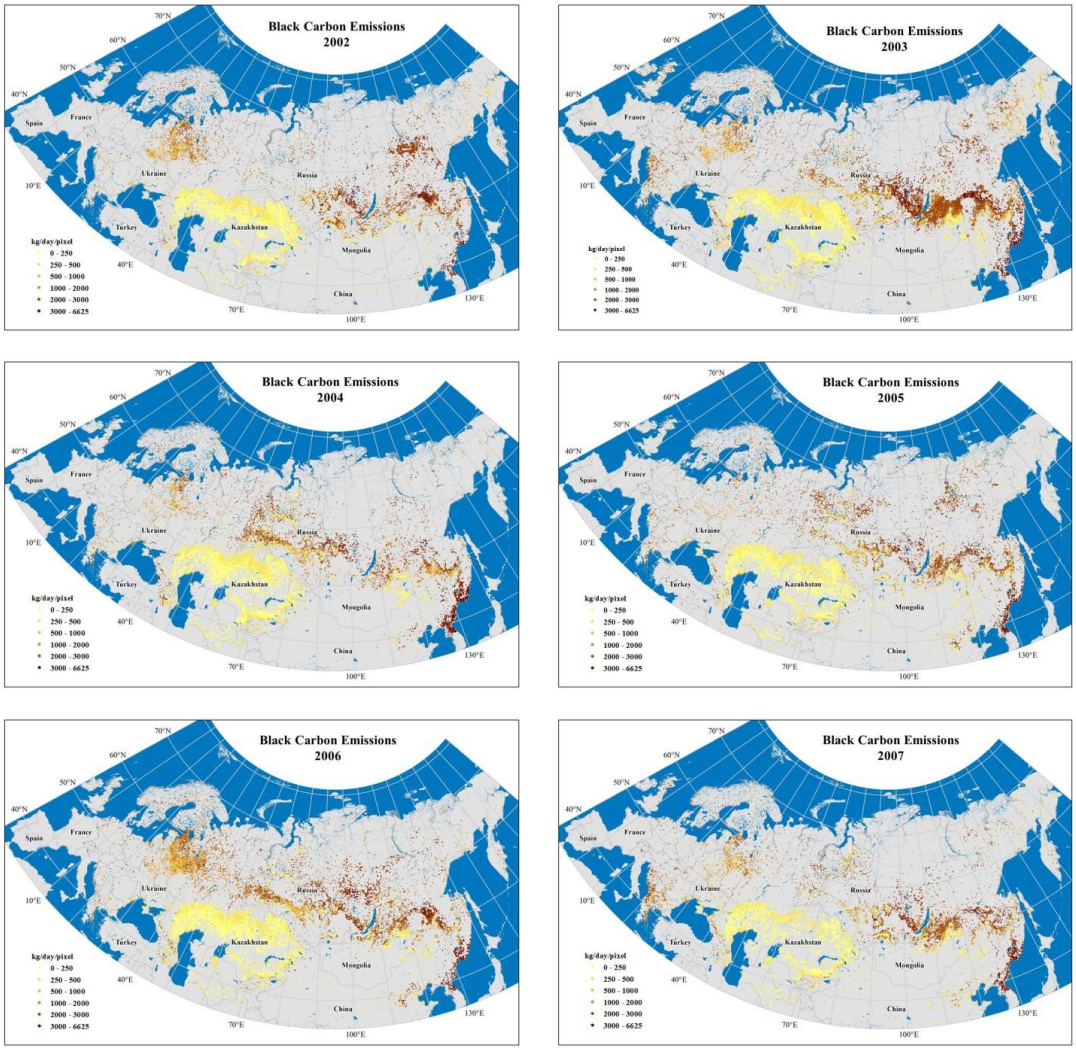

Figure 3. Daily BC emissions in Northern Eurasia at a 500 m × 500 m resolution from 2002-2013.

Geosci. Model Dev. Discuss., doi:10.5194/gmd-2016-89, 2016
Manuscript under review for journal Geosci. Model Dev.
Published: 21 April 2016

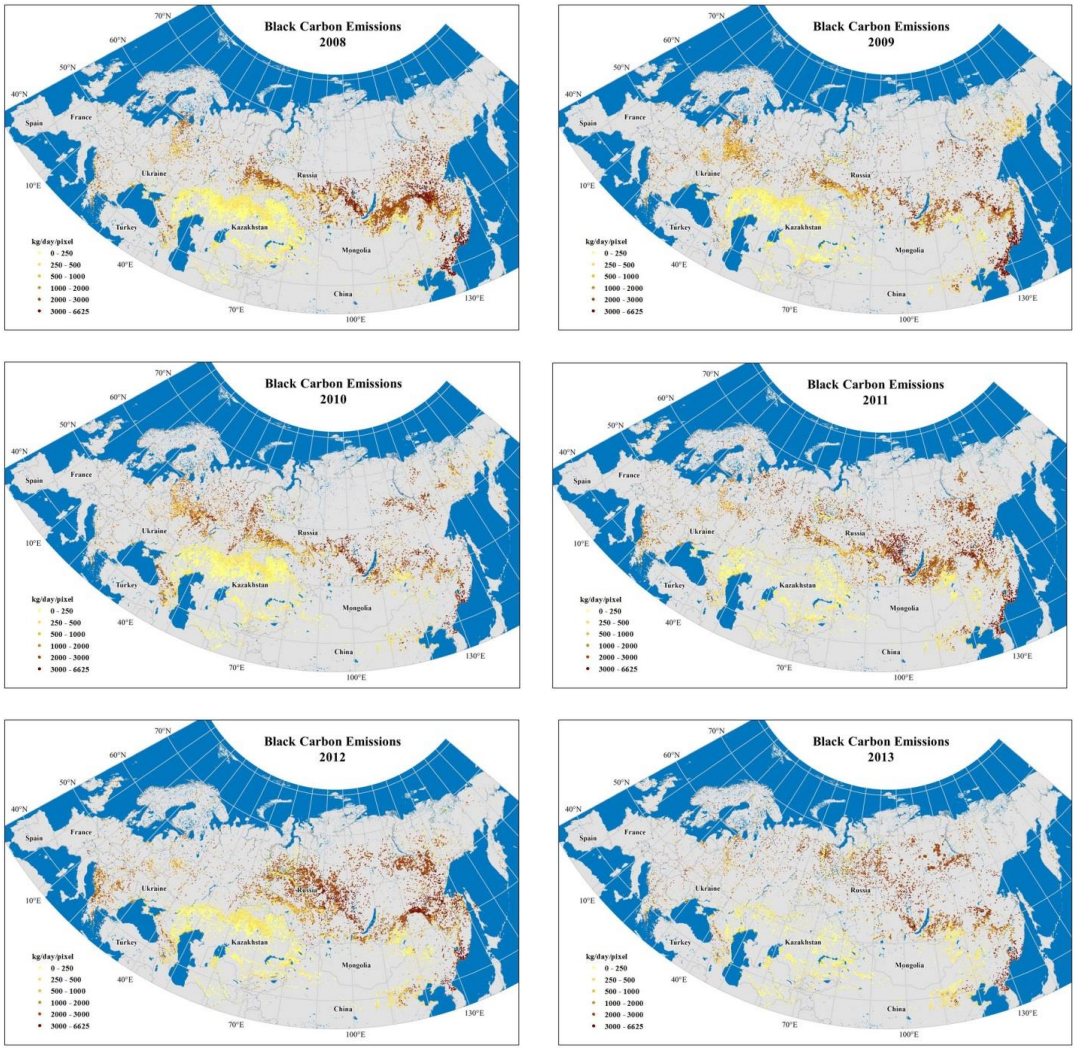

Figure 3. Daily BC emissions in Northern Eurasia at a 500 m × 500 m resolution from 2002-2013 (continued).

Geosci. Model Dev. Discuss., doi:10.5194/gmd-2016-89, 2016
Manuscript under review for journal Geosci. Model Dev.
Published: 21 April 2016

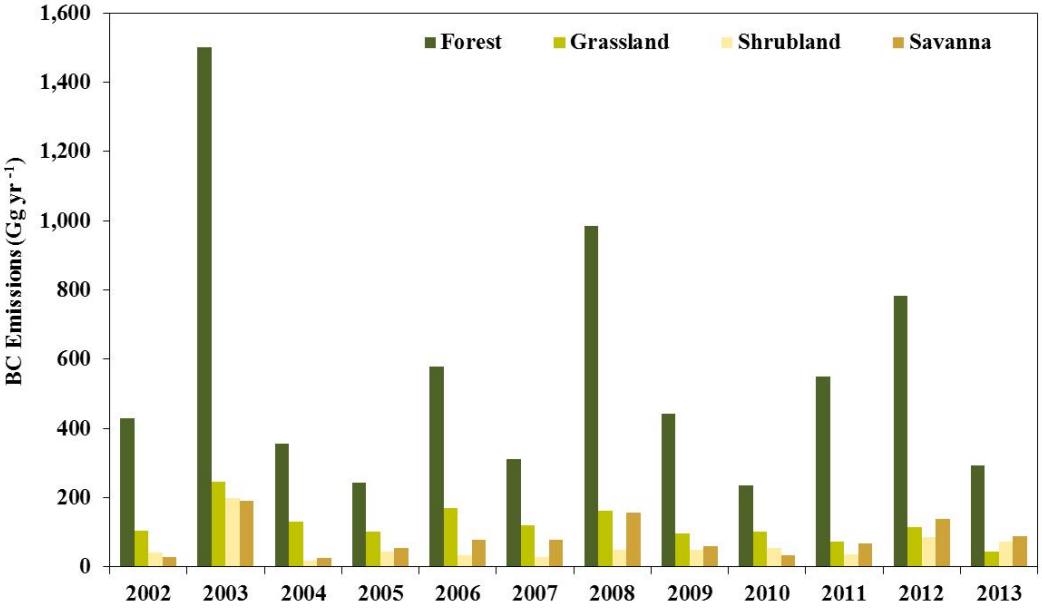

Figure 4. Interannual variability of BC emissions for different land cover types in Northern Eurasia from 2002-2013.

Geosci. Model Dev. Discuss., doi:10.5194/gmd-2016-89, 2016
Manuscript under review for journal Geosci. Model Dev.
Published: 21 April 2016

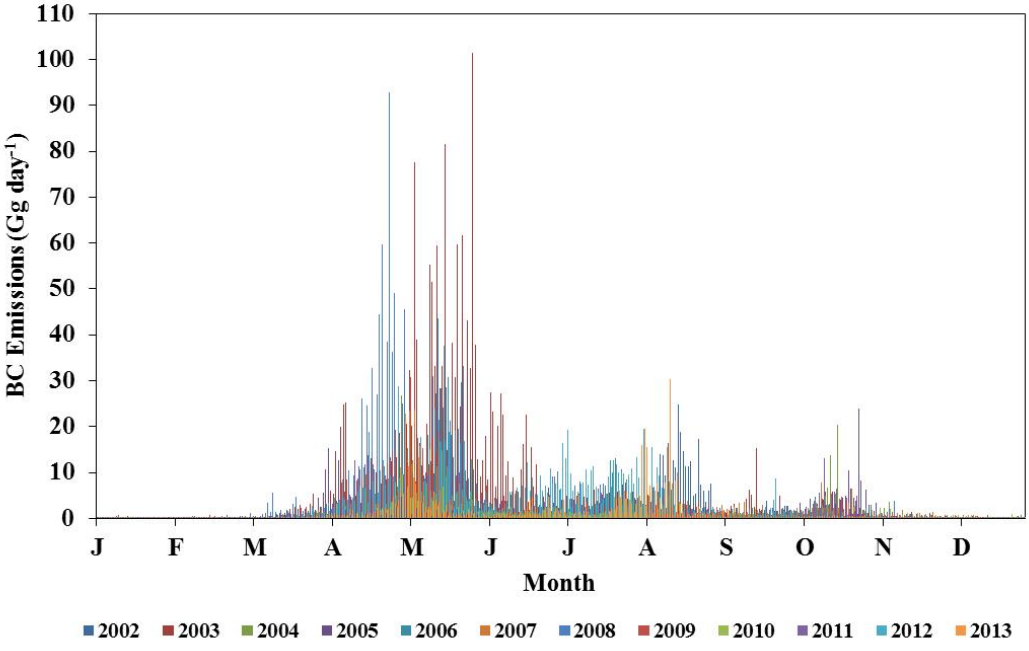

Figure 5. Daily BC emissions in Northern Eurasia from 2002-2013.

Geosci. Model Dev. Discuss., doi:10.5194/gmd-2016-89, 2016
Manuscript under review for journal Geosci. Model Dev.
Published: 21 April 2016

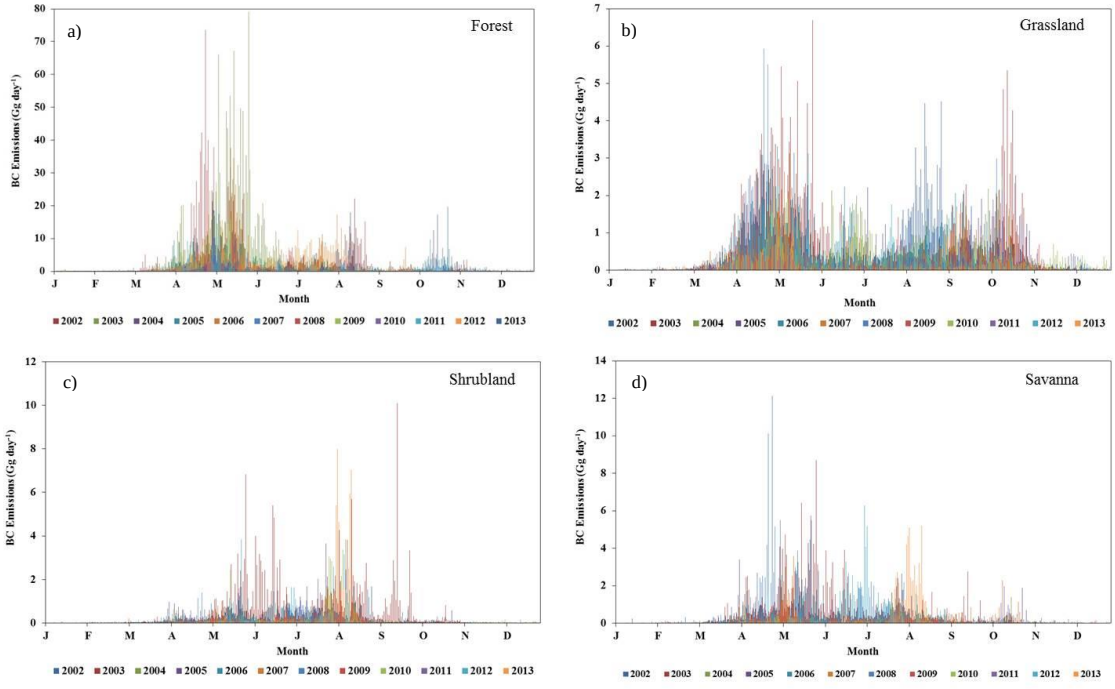

Figure 6. Daily BC emissions in different land cover types in Northern Eurasia from 2002-2013. Note the differences in the Y-axis scales of BC emissions from fires in different land cover types.

Geosci. Model Dev. Discuss., doi:10.5194/gmd-2016-89, 2016
Manuscript under review for journal Geosci. Model Dev.
Published: 21 April 2016

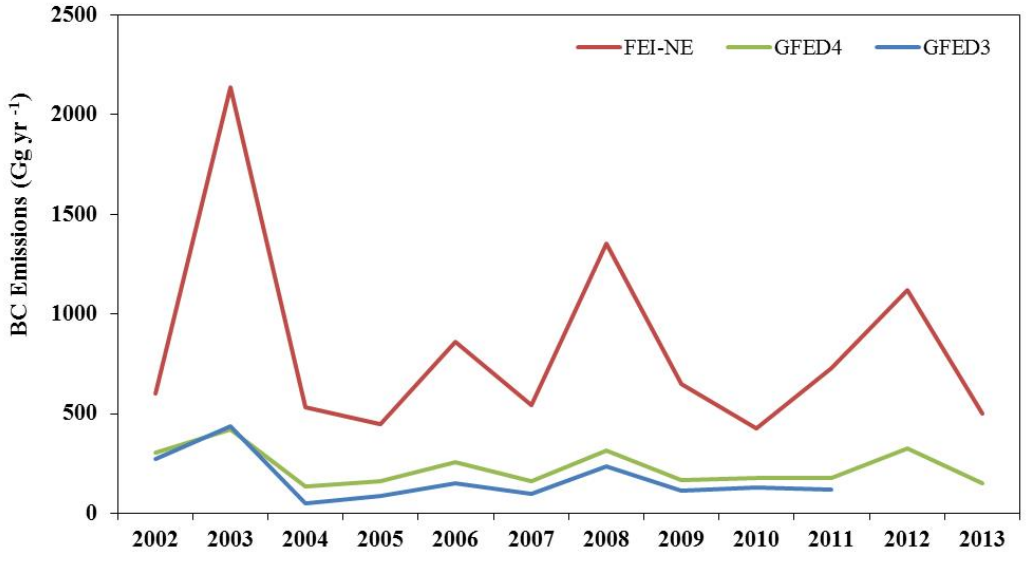

Figure 7 Comparisons of annual BC emissions from biomass burning in Northern Eurasia from 2002-2013 estimated by FEI-NE, GFED4, and GFED3.

Geosci. Model Dev. Discuss., doi:10.5194/gmd-2016-89, 2016
Manuscript under review for journal Geosci. Model Dev.
Published: 21 April 2016

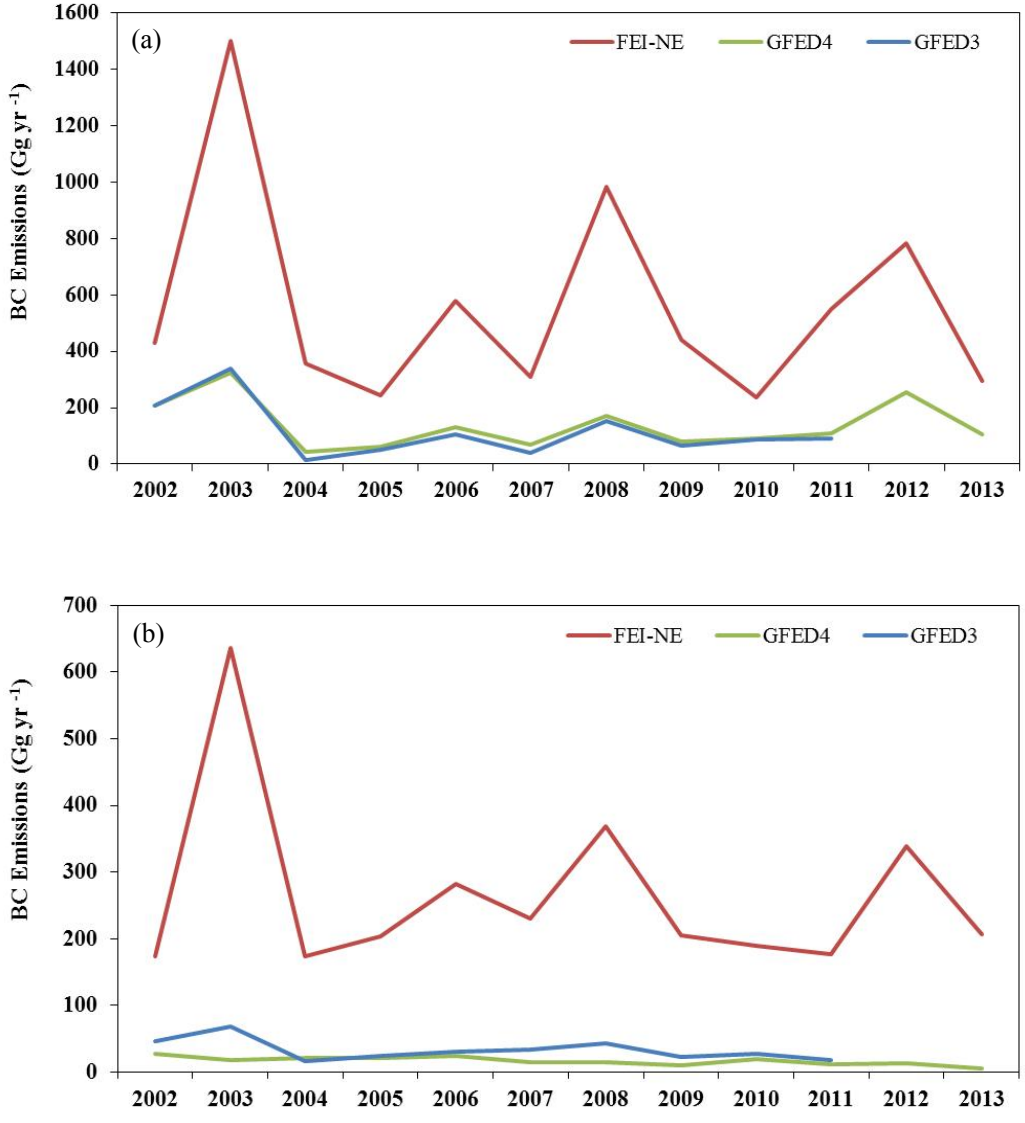

Figure 8. Comparisons of annual BC emissions from (a) forest and (b) non-forest fires in Northern Eurasia for FEI-NE, GFED4, and GFED3 from 2002-2013.